J. Plasma Fusion Res. SERIES, Vol. 3 (2000) 440–443

Development of the Real-time Image Data Acquisition System for Observing the Plasma Dynamic Behavior of LHD Long-pulse Discharges

SHOJI Mamoru*, YAMAZAKI Kozo and YAMAGUCHI Satarou
National Institute for Fusion Science, Toki 509-5292, Japan

(Received: 18 January 2000 / Accepted: 6 April 2000)

Abstract

The experimental results of plasma dynamic behavior and impurity radiation profiles measured with tangentially viewing CCD cameras in Large Helical Device (LHD) are reported. The two dimensional profile of visible line emission from oxygen, carbon, helium and hydrogen has been measured. The cameras observed magnetic island structure in the plasma periphery and divertor magnetic field line structure. These structures are consistent with the calculations obtained by a multi-filament model. The image data taken with these cameras will give useful information for the analysis of the effect of the magnetic island on impurity transport and for designing a closed divertor configuration planned in Phase II. The image data acquisition system using data compression technique (MPEG-2) will be also described.

Keywords:
image data acquisition, MPEG, CCD camera, long-pulse discharge, impurity measurement

1. Introduction

Charge Coupled Device (CCD) cameras are widely used for observing plasma dynamic behavior, impurity radiation profiles and plasma-wall interactions, etc [1-4]. The image data taken with the cameras give much useful information. However, huge data storage system is needed because of the output signal from many pixels on the CCD arrays. When we used a standard video camera (NTSC), a video data stream (~100 Mbps) is generated, corresponding to (125 Mbytes/shot!) when the camera monitor plasma discharge for 10 seconds. Video Tape Recorders (VTR) have been widely used for image data acquisition. This analog recording system has some disadvantages, i.e., the recorded images deteriorate compared to the original images and tracking noise is inevitable. Furthermore, we cannot access the data at random, which is inconvenient for flexible data analysis and efficient plasma experiments.

Recently, image data compression technique such as JPEG and MPEG has been developed in the Internet technology. We applied the compression technique to the data acquisition of plasma images in LHD. In the next chapter, the image data acquisition system will be shown. We will briefly explain the data compression technique (MPEG-2) in chapter 3, and give the dependence of the image quality on compression in chapter 4, and two-dimensional profiles of impurity line emission acquired with this system in chapter 5.

2. Tangentially Viewing Cameras and Image Data Acquisition System

In plasma discharge experiments in LHD, tangential viewing CCD cameras have been used as useful apparatuses for monitoring plasmas. One camera is mounted in the tangential port (7-T), and four cameras

*Corresponding author's e-mail: shoji@LHD.nifs.ac.jp

(SONY DXC-LS1) with interference filters are installed in another tangential port (6-T). We can choose four interference filters from six ones (OII: 442.5 nm, CIII: 465.4 nm, CII: 426.7 nm, HeI: 587.8 nm, HeII: 468.6 nm and H_α: 656.6 nm) for these cameras. The video signals from the cameras are integrated with a video multiplexer. The video signal is converted to an optical signal with a converter for avoiding electric noises. We have stored the video signal by a video tape recorder (SONY SVT-S5100). To overcome the defects of the analog recording, we newly introduced a Video On Demand (VOD) system during the third experimental campaign. Figure 1 shows the configuration of the VOD system. The video signal is received by an MPEG-2 encoder board (FutureTel PrimeView-Duet) installed in a VOD encoder server. The data of the video sequence is compressed by an MPEG-2 image data compression technique and is stored in hard disks. The plasma video image data can be easily accessed from a client terminal in the Local Area Network (LAN) for a LHD control data processing system [5]. We have determined the sequence for plasma heating devices and the gas fueling rate for the next plasma shot by considering the plasma images and experimental results measured with many plasma diagnostics. The camera system has also been useful for controlling the gas fuelling rate in long-pulse discharges. Since there are no abrupt plasma disruptions in helical systems, we can easily control the plasma density by optimizing the fuelling rate manually while monitoring the plasma. Our final goal is to sustain plasmas for several hours. In this experiment, the real-time image data acquisition is essential, unless extraordinary huge buffer memories for storing the image data are needed. The VOD system can encode and store the image data in real-time (less than a few hundred msec), contributing to efficient image data acquisition at a reasonable cost.

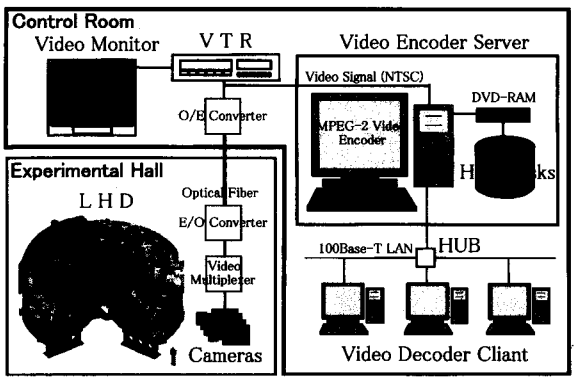

Fig. 1 Configuration of the VOD system for monitoring LHD plasmas.

3. Image Data Compression Technique

The image data compression technique MPEG-2 is the second phase of MPEG (Moving Pictures Experts Group) standard [6]. It provides higher-quality encoding and is designed for providing higher-resolution video. MPEG-2 is a lossy compression in which some of the original data is lost. Although image fidelity may be compromised, up to 95 percent of the data representing a particular image may be discarded without an apparent loss in resolution. Images are compressed by Discrete Cosine Transform (DCT), which is a form of encoding to transform spatial information, typically an 8×8 block of pixels, into digital frequency information. In this process, high-frequency components are reduced, leaving a softer picture but offering greater compression. An MPEG-2 video sequence consists of a Group of Pictures (GOP) which is a series of one or more pictures intended to allow random access into the video sequence. A GOP is composed of three kinds of frame: I-, P- and B-frame. I-frame is a reference picture using only the information present in the image itself and coded using only the DCT compression. P-frame is coded from the information contained in the nearest previous reference frame: either an I-frame or another P-frame. B-frames utilize information from both previous and future frames.

4. Optimization of Image Data Compression

Before applying the MPEG-2 standard to plasma image data acquisition, we optimized the video sequence bit rate acquired in the VOD system. Figure 2 shows the time evolution of the images of the impurity radiation observed with the cameras mounted in the 6-T port. Figure 2 (a), (b) and (c) are the images in the case where the video bit rate is 0.58, 2.31 and 5.77 Mbps, respectively. Prominent block noises appear in the first frame in the lowest video bit rates. The block noise is a typical noise appearing in compression process by DCT. The noise diminishes as the progress of frames, which is ascribed to the fact that the plasma shape becomes steady as the progress of time. As a result, the accuracy of the prediction of the images from I-pictures becomes higher, leading the reduction of the noises under the limitation of a specified video bit rate. Considering the quality of the plasma images in the plasma start-up phase and comparing with the video images recorded in

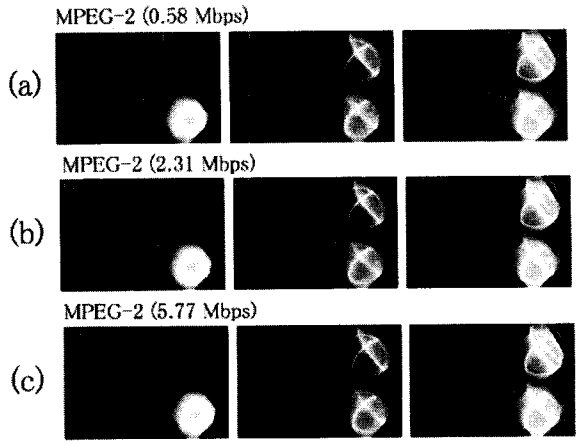

Fig. 2 Dependence of the video streaming bit rate on the plasma images taken by the CCD cameras installed in 6-T port for (a) 0.58, (b) 2.31, (c) 5.77 Mbps, respectively.

the VTR, the optimized video bit rate is set to be 5.77 Mbps. Consequently, we have succeeded in compressing the video image data into a reasonable size which is as small as about 1/17 of that without compression.

5. Measurement of Impurity Emission Profiles

5.1 Magnetic Island Structure

We used the image data acquisition system for storing impurity emission profiles measured with the four cameras in the 6-T port. We have observed many interesting plasma images. For an example, the double layer structure of the line emission from carbon ions (CII) in the plasma periphery in a plasma start-up phase is shown in Figure 3 (a). We have already found the presence of an m(poloidal mode number) = 1 magnetic island in the plasma periphery by magnetic surface measurement using a fluorescent technique under high magnetic fields [7]. We thought that the double layer was ascribed to the effect of the magnetic island: trapped carbon ions in the island spread along the magnetic field lines to form the emission profile along the magnetic island. We calculated the three dimensional magnetic island structure by a multi-filament model (HSD code) including the error field which can explain the experimental results of the magnetic surface measurement. Figure 3 (b) illustrates the calculated structure seen from the 6-T port, which agrees with the experimental result. We have confirmed the presence of the double layer structure by another camera in the 7-T port. These experimental results show

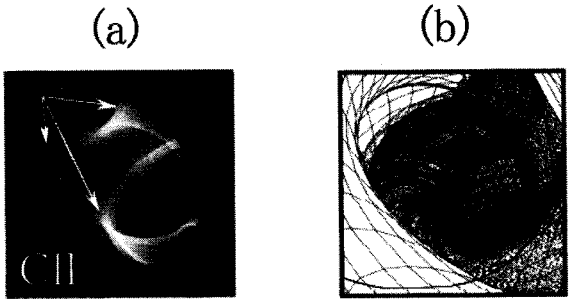

Fig. 3 (a) Radiation profile of carbon ions (CII) observed in the plasma start-up phase. (b) Calculated magnetic island structure seen from the tangential port (6-T).

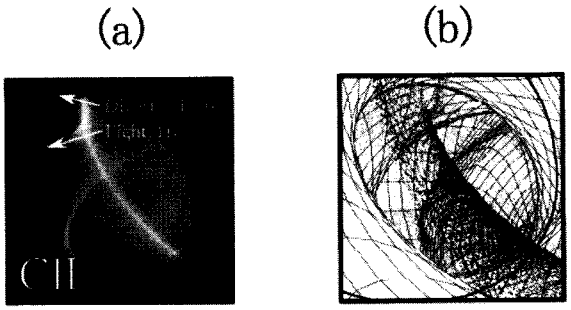

Fig. 4 (a) Radiation profile of carbon ions (CII) observed in an NBI-heated plasma. (b) Calculated divertor magnetic field line configuration seen from the tangential port (6-T).

that the magnetic island structure can be measured during the plasma discharge by using the tangentially viewing cameras. The camera system will contribute the investigation of impurity and particle transport in a Local Island Divertor (LID) configuration in LHD.

5.2 Divertor magnetic field line structure

Divertor magnetic field line structure is essential for particle and impurity removal in long-pulse or steady state plasmas. It is important to clarify the structure of the divertor plasma before designing the closed divertor configuration planed in Phase II in LHD. The position of the divertor plasma has been locally measured with an electrostatic probe. Formation of the divertor structure, however, has not yet been clarified in detail. In NBI-heated plasmas, we observed a clear light trace which firstly appeared in the third experimental campaign as shown in Figure 4 (a). We though that the light trace was ascribed to the formation of the plasma along the divertor magnetic field lines. Using the multi-filament model, we calculated the three dimensional

structure of the divertor magnetic field lines. Figure 4 (b) shows the calculated image of the field lines seen from the 6-T port, which agrees with the measured image (Figure 4 (a)). The calculated image seen from the 7-T port also proves the consistency with the image observed by the camera in the 7-T port. Consequently, we have succeeded in clarifying the presence of the divertor structure from the image taken with the tangentially viewing cameras. It is expected that the camera systems give us useful information on impurity transport and the divertor plasma physics for achieving steady-state plasma operation.

6. Summary

The image data compression technique (MPEG-2) has been successfully applied to acquisition of the plasma image data by optimizing the acquired video bit rates. The image data have been compressed to be a reasonable size (about 1/17 of that without compression). The tangentially viewing CCD cameras observed the magnetic island structure in the plasma start-up phase and the divertor structure in the NBI-heated plasmas. These structures are in agreement with images of the 3-dimensional magnetic field line structure calculated by the multi-filament model including the error field. These image data are expected to be useful for investigating the effect of the magnetic island on impurity transport in the plasma periphery and for designing the closed divertor configuration to achieve steady-state plasmas in the future.

Acknowledgements

The authors are grateful to Mr. Nagae for his contribution to construction of the image data acquisition system, and we would like to acknowledge the members of LHD experimental groups for their collaboration in plasma discharge experiments.

References

[1] S.J. Zweben *et al.*, Phys. Fluids B 1 **10**, 2058 (1989).
[2] F.Sardei *et al.*, J. Nucl. Mater. **241–243**, 135 (1997).
[3] D.G. Nilson *et al.*, Rev. Sci. Instrum. **70**, 738 (1999).
[4] R.J. Maqueda *et al.*, Nucl. Fusion, **39**, 629 (1999).
[5] S. Yamaguchi *et al.*, J. Plasma Fusion Res. **73**, 335 (1997).
[6] http://drogo.cselt.stet.it/mpeg/
[7] M. Fujiwara *et al.*, Proc.26th EPS Conf. on Contr. Fus. and Plasma Phys., Mastricht (1999).